Failure analysis study of a tower crane collapse due to height increasing

Análise do colapso de uma grua torre devido ao incremento da altura

Francisco Castro[1] | Nuno Viriato Ramos[1] | Francisco Queirós de Melo[1] | Pedro Moreira[1] | Mário Vaz[2,1]

[1]INEGI – Instituto de Ciência e Inovação em Engenharia Mecânica e Engenharia Industrial, Portugal
fcastro@inegi.up.pt; nviriato@inegi.pt; fmelo@inegi.up.pt; pmoreira@inegi.up.pt
[2]FEUP – Faculdade de Engenharia da Universidade do Porto (FEUP), Portugal, gmavaz@fe.up.pt

Abstract

The failure of a large tower crane can cause high economic losses and serious injuries or fatalities, that's why it's extremely important to identify, not only the causes of its collapse for the attribution of responsibilities, but also and specially focusing on the prevention of new disasters. This paper aims to study and investigate the main causes of the accident and its reconstruction by sequenced collapse stages. Static and dynamic computational simulations were performed to understand the main changes of the structure dynamic behavior due to the height increasing and eventual material changes, which was not contemplated in the manual. It was possible to conclude that the main cause for the accident was due to the excitation of natural frequencies of the structure associated to a pendulum effect of the suspended loads. The changes in the flexibility of the structure due to the increase in height and its dynamic interaction with the oscillations of the suspended load are presented and discussed.

Keywords: Experimental mechanics, Computational Simulations, Tower Crane Collapse, Forensic Engineering

Resumo

A queda de uma grua torre de grande porte pode causar elevados prejuízos económicos e ferimentos graves ou mortais, por isso é extremamente importante identificar não só as causas do seu colapso para a atribuição de responsabilidades, mas também e especialmente contribuir para a prevenção de novos desastres. Este trabalho tem como objetivo estudar e investigar as principais causas do acidente e realizar a sua reconstrução por etapas sequenciadas até ao colapso. Simulações computacionais estáticas e dinâmicas foram realizadas de modo a estudar as principais alterações no comportamento dinâmico da estrutura devido ao aumento de altura e eventuais alterações de material, que não estejam contemplados no manual. Foi possível concluir que a principal causa do acidente foi a excitação das frequências naturais da estrutura associada a um efeito pêndulo de cargas suspensas. São apresentadas e discutidas as alterações na flexibilidade da estrutura devido ao aumento da altura e a sua interação dinâmica com as oscilações da carga suspensa.

Palavras-chave: Mecânica experimental, Simulações Numéricas, Colapso de Grua Torre, Engenharia Forense

1- INTRODUCTION

A tower crane is a rotatable cantilever jib on the top of a steelwork tower mounted on a construction site, which its main function is moving loads at height. Tower cranes play a critical role in the construction industry, enabling the efficient lifting and transportation of heavy materials at large heights. Due to the level they can be mounted and their unique operating conditions, they are subject to several forces, with and without moving loads and exposed to adverse weather conditions.

Despite their robustness, tower cranes are not immune to failures, and when such failures occur, they can present devastating consequences to human lives, infrastructures and the surrounding environment. According to reports and published statistics, between 2000 and 2008, approximately 1125 crane accidents have been registered worldwide, with 780 fatalities [1, 2, 3]. Furthermore, accidents occurring with tower cranes represented approximately 22 % of all types of cranes accidents [4].

Therefore, understanding the causes and mechanisms under these collapses is of utmost importance to prevent future incidents and ensure the safety of workers and the public [5, 6, 7, 8]. The main causes for tower crane accidents can be grouped into the following categories: tasks due to assembly or disassembly of the crane (34%); misuse (7%); extreme weather conditions (18%); proximity hazards; foundations problems (2%); mechanical or structural failures (5%), electrical/control problems (1%) and unknown causes (33%) [9, 10, 11].

The investigation carried out throughout this paper focuses on a tower crane collapse that occurred because of an increase in its height. The decision to extend the crane's height was driven by the requirements of the construction project. For the examination of this accident in detail, a site and equipment inspection were prepared, this combining with analytical techniques and also with static and dynamic numerical simulations. Ultimately, this research aims to pave the way for improved design considerations, operational guidelines, and safety protocols in the construction industry to prevent similar incidents and ensure the well-being of construction personnel and the public.

2- THE ACCIDENT

2.1. Tower crane

The crane involved in this accident is a SOMA SGT 6012TL and according to the data provided by the manufacturer, this is a fixed tower crane characterized by an available maximum height of 42 meters and a maximum boom length of 60 meters.

Regarding the information collected by the investigation team, the crane had a height of 60 meters and a boom length of 45 meters (Figure 1a). However, besides the boom length of 45 meters

being contemplated in the manual of the manufacturer (Figure 1b), the height it's not in accordance. Also, the constructor installed a counterweight of 15 tones, 3 tones above the value mentioned in the manual. The tower crane foundation was totally fixed to the construction ground site (Figure 1c) and no connection was installed between the crane body and the building structure.

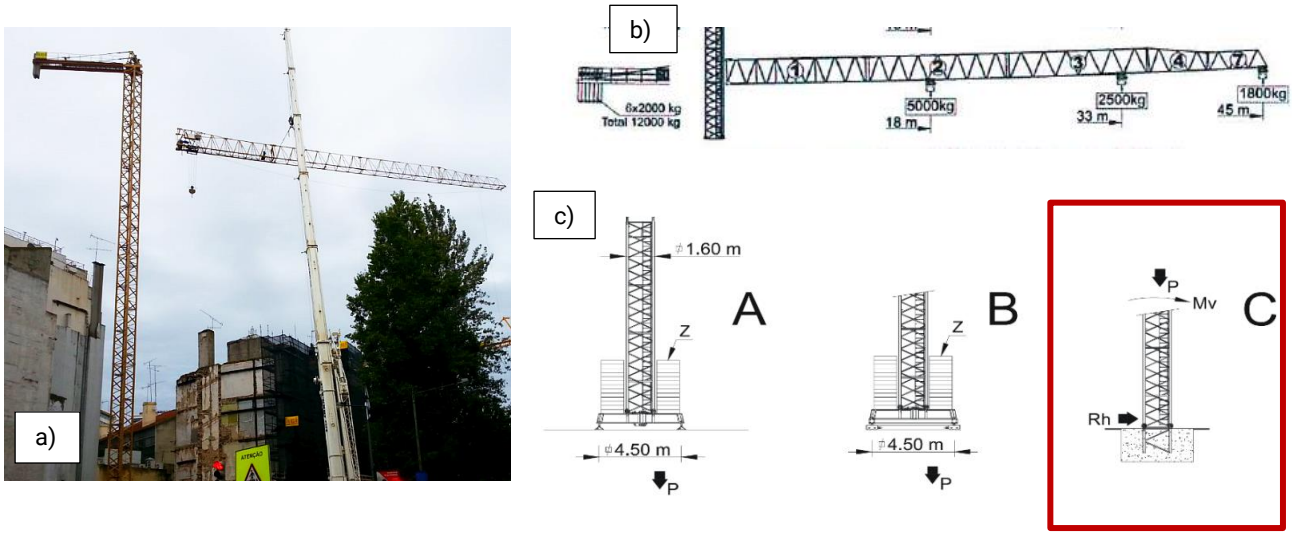

Fig. 1 | a) Tower crane being assembled; b) Admissible loads in the boom and counter boom; c) Types of foundations and foundation used.

2.2. Collapsing

Regarding the accident description, the horizontal section (counter-boom and boom) collapsed, as result of the sequential rupture of the slewing unit bolts which were being subjected to high tensile forces. During the bolts failure, the crane upper part rotated around the horizontal axis perpendicular to the crane structure and twisted (Figure 3 and Figure 4), falling down to the side of the counter-boom, i.e., into the direction of the crane's center of gravity, colliding against the top of neighboring buildings (Figure 2, Figure 5 and Figure 6) Unexpectedly the boom had an upward movement, despite the fact of having a suspended load. The crane tower remained erect and without severe structural damage.

The following representations aim to reconstruct the several stages of the tower crane collapse, according to the crane final position, data collected from the inspections and witness reports.

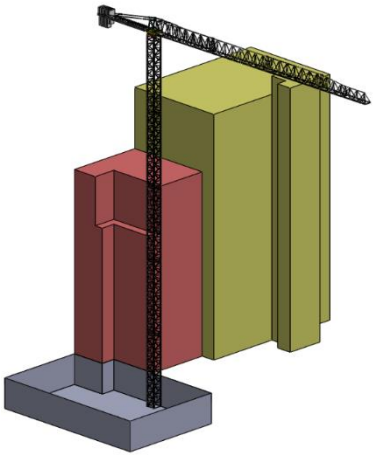

Fig. 2 | Tower crane and surrounded neighboring buildings.

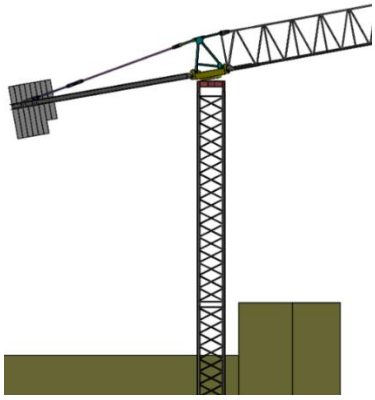

Fig. 3 | Rotation of the horizontal section, due to the failure of swing unit bolts.

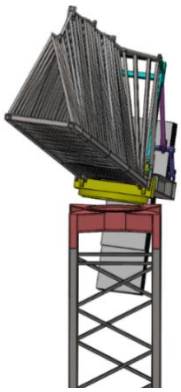

Fig. 4 | Rotation and twisting of the horizontal section of the crane.

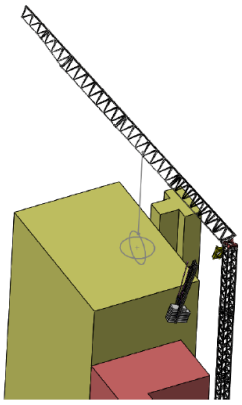

Fig. 5 | Falling of the slewing unit, counter-boom and boom.

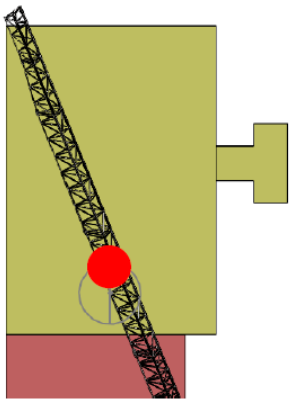

Fig. 6 | Final position of the boom and cables on the top of neighboring buildings (top view).

As mentioned previously, after the accident, the tower shows to be still and fixed and without its horizontal structure (Figure 7), which fell down, impacting the top of the building close to it (Figure 8).

The slewing unit of the crane allows the boom to rotate because of its internal geared pinion/wheel driven by two electric motors (Figure 9). This unit is attached to the crane's tower by 48 bolts tightened with a pre-set torque, which started do fracture during the rotation (Figure 10). Some of them were projected away, while other remained in the respective holes. As can be seen the fracture

Fig. 7 | Tower crane after accident.

Fig. 8 | Final position of the Boom after falling on top of a neighbor building.

Fig. 9 | Slewing unit of the crane and its motors.

Fig. 10 | Detailed of the screw cross section evidencing brittle fracture.

section presents two distinct aspects: a lighter area corresponding to the final rupture and one darker, due to the existence of a propagated crack with corroded surfaces, a factor potentiating a faster crack growth velocity prior to the accident.

The visual inspection to the inner geared ring of the slewing unit, allowed the identification of at least two cracks close to the teeth root fillet, in a zone weakened by bolt hole machining (Figure 11). On the other hand, a detailed inspection revealed some irregularity marks where the pinion works (Figure 12), whose origin can be associated with the relative movements due to backlash between the two parts.

Following the initial inspection and presentation of the problem, concerns emerged regarding the assembly and maintenance of the crane's main components. These concerns served as a catalyst for conducting a more comprehensive and meticulous analysis aiming the identification of the primary causes for the accident.

Fig. 11 | Detail of the rack where two fractures are identified.

Fig. 12 | Detail of the top of the crane tower where irregular marks are visible.

2.3. Possible causes

Based on the information gathered from the accident site and witnesses' testimonies, there are some circumstances that potentially contributed to the accident occurrence.

1) Mounting error; according to the information provided and to the instruction manual, the crane should not reach/exceed a 60 meters height. However, it was found that it was mounted a conical section at the base of the tower which allows, according to the

manufacturer, to support the structure and respective use of the crane at least for static responses.

2) Maintenance; according to the findings, maintenance was carried out regularly and there was never an irregular situation that could jeopardize the integrity of the crane.

3) Misuse; it was not possible to determine whether the crane performed any of the non-recommended uses.

4) Crane motors; the regular maintenance of the crane includes checking the mechanical part of the crane including the motors and there was not any record of irregularities.

5) Irregularities verified at the top of the tower; the presence of marks indicating the absence of lubrication mass raises concerns regarding potential misalignment of the pinion, which could lead to compression forces through contact in that area. Additionally, the presence of wear patterns resembling a cycloid suggests the possibility of a backrest being present during the movement. Consequently, these marks can be attributed to the dynamic forces associated with the collapse.

6) Rack fractures; these fractures were not identified in the maintenance carried out to the crane. Its origin is related to irregular requests resulting from a defective gearing. If the pinion and rack axes are not parallel, there may be a variation in the gear middle-axes along the tooth width. Thus, part of the pinion tooth would get a little more inside the teeth of the rack, which would rise to an abnormal wear of the gear surface. Besides, the tooth flank is slightly concave, as would be expected if there is a lack of parallelism between the pinion and the rack.

7) Connection bolts of the slewing unit; it was not checked how the manufacture assembled that unit or how regularly the bolted connection was inspected.

Despite an analysis of all potential causes, no sound evidence of the accident's likely causes has been found. Consequently, to further investigate and shed light on the circumstances surrounding the accident, it became imperative to conduct a thorough static and dynamic analysis.

3- AN ANALYTICAL APPROACH

3.1. Main efforts and simple design procedures

Major problems in the design of crane truss-type structural modules (beam and column) deal with compression forces, rather than tensile efforts. If these are combined with bending moments, they easily potentiate the buckling of each structure's single member, leading to a major collapse of the whole structural module. In this section, simple but essential design rules to a safer structure are reminded. Considering the following example, a truss-type column having a square section (Figure 13).

The first assessment for the structure integrity consists in checking it for limit axial

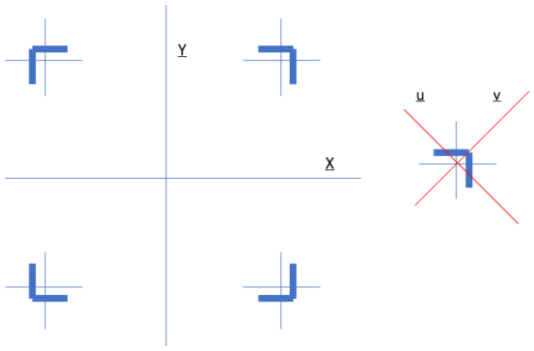

Fig. 13 | Truss-type column with a square section.

compression load, which can lead to structure breakdown due to buckling. In case of a truss type column, as these are frequently adopted in crane design, the concern goes to check the maximum allowable compression force that the column can withstand for buckling. This is achieved by obtaining the moments of inertia and the radius of gyration of the column cross section as an assembly of main beam integrating the tower structure. By evaluating the column slenderness, it is necessary to check for the allowable axial force, which leads to the maximum compression load of the section.

A second procedure consist in checking separately how each single beam of the tower withstands the assigned axial load. Now, the slenderness of each beam depends on the radius of gyration (eventually obtained for transverse section principal axes that are differently oriented if compared with the principal ones of the assembled section). The application of the buckling design criterion is now useful to recommend the safe simple beam length pitch for each cell, where the node fixture can range between the perfectly built-in ends (not realistic) and the perfect pinned ends (also somewhat optimist), where at this option it is advisable to follow design codes.

3.1.1. Example

Let´s suppose a square section of 300 mm where main single beam members are 80×8 L-beams. The truss beam has a pitch module of 1000 mm, where each single beam is assumed to be fixed as having built-in ends.

The neat transverse section area of the assembled column is $A_{tot} = 4 \times 160 \times 8 = 5120\, mm^2$. The transverse inertia moment is approximately given by $I_{xx} = I_{yy} = 4 \times 160 \times 8 \times 1502 = 1{,}152 \times 10^{8}\, mm^4$. The radius of gyration is $r_g = (1{,}152 \times 10^{8})/\,5120) \times 0{,}5 = 150\, mm$.

Now, considering a global height of 10 meters (10000 mm); for a built-in end only, the equivalent buckling length is 20000 and the slenderness is $\lambda = \frac{20000}{150} = 133$.

According with the graphic presented in Figure 14[12], the global reduction factor is about 0,45 for a slenderness λ= 133. (relative slenderness is real value divided by 100)

If the yield material allowable stress is 240 MPa (steel ST370), then the critical load is (not considering the transverse shear effect),

$$F_{crit} = 0{,}45 \times 240 \times 5120 = 553\, kN = 56\, Tones \quad (1)$$

Now, let's assess the critical load for each single L-beam. Considering the minor section moment of inertia in bending (as indicated by the small figure near the main tower section in

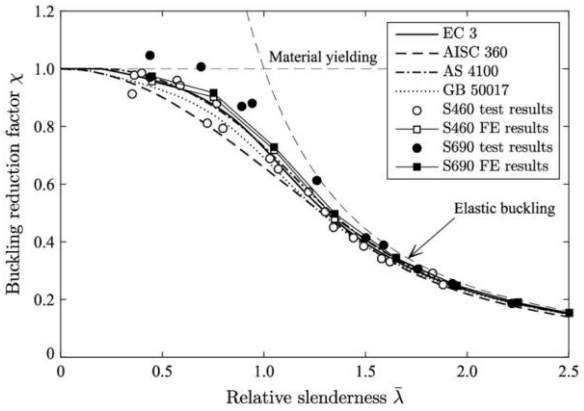

Fig. 14 | Relation between relative slenderness and the buckling reduction factor [12].

Figure 13), the corresponding radius of gyration is 15,5 mm (about axis u).

Assuming the same slenderness, now to a single beam as the one of the global trussed columns, the equivalent length for each beam would be,

$$L_{1beam} = 15{,}5 \times 133 = 2062\ mm \tag{2}$$

This would be the maximum recommended single cell pitch length to avoid isolated buckling for each single beam. Naturally the adoption of smaller distance would lead to a safer design.

3.2. Buckling analysis by non-linear geometric model

The problem of structural instability through finite element techniques, needs the adoption of non-linear geometric modelling. This arises from the fact that strain expressions do not follow linear functions, which imposes the use of incremental solutions bearing on the concept of "tangent" stiffness matrices. These matrices employ a linear formulation, but are only valid for each load increment step during the problem-solving solution.

Considering the example of an elementary fragment dx of a main beam subjected to axial compression load, this beam undergoes a lateral displacement by bending resulting from buckling (Figure 15). Then, each elemental beam fragment projects a displacement given by,

$$\Delta dx = dx(1 - cos\ \theta) \tag{3}$$

and the corresponding non-linear geometric deformation as result of this loading mode is (being negative, due to the compression force),

$$\varepsilon_{nlg} = -\frac{\Delta dx}{dx} = -1 + cos\ \theta \tag{4}$$

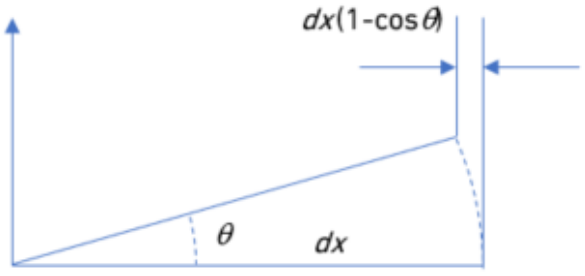

Fig. 15 | Lateral displacement of a beam subjected.

Since θ is generally a small angle, developing the previous expression in a Taylor expansion, gives,

$$cos\,\theta = cos\,0 + \theta(cos\,\theta)'_{\theta=0} + \frac{\theta^2}{2!}(cos\,\theta)''^{\theta=0} + \cdots \cong 1 + 0 - \frac{\theta^2}{2!} = 1 - \frac{\theta^2}{2} \quad (5)$$

The non-linear geometric deformation is,

$$\varepsilon_{nlg} = \Delta dx/dx \simeq -\frac{\theta^2}{2} \quad (6)$$

As depicted in Figure 15, θ can be associated with the element slope (for small values); which is,

$$\theta = \frac{dy}{dx} \quad (7)$$

Therefore, the final expression of the non-linear geometric deformation is then,

$$\varepsilon_{nlg} = -\frac{1}{2}\left(\frac{dy}{dx}\right)^2 \quad (8)$$

With this expression, it's possible to calculate the axial displacement due to bending of the beam by effect of the buckling. Usually, the displacement due to purely axial strain by compression force may be discarded, as it represents a much smaller contribution compared with bending by buckling. Then, the axial displacement is given by,

$$u_{axnlg} = \int_0^{L_0} \varepsilon_{n\,lg} \quad dx = -\frac{1}{2}\int_0^{L_0}\left(\frac{dy}{dx}\right)^2 dx \quad (9)$$

It should be noted that for positive transverse displacements of the beam (by bending), the projected length reduces, resulting in a negative value for this displacement.

In the formulation of a finite element beam, the previous expression is an important contribute to setup a stiffness matrix where buckling effects are included. Let's consider the transverse displacement formulation by nodal displacements and interpolation shape functions, as frequently proceeded with this methodology,

$$y(x) = [N(x)]\{y_e\} \quad (10)$$

where y(x) refers to the beam transverse displacement, $[N(x)]$ is the shape function matrix and $\{y_e\}$ is the nodal displacement vector, ensuring the continuous definition of the transverse displacement by interpolation with the shape functions. In the case of a Euler-Bernoulli beam model, the relevant strain for bending deformation is the curvature, given by the second derivative function of y(x). The constitutive equation which associates the bending moment with the curvature is as follows,

$$M(x) = EIy''(x) = EI[N''(x)]\{y_e\} \quad (11)$$

When evaluating a small strain energy variation for bending deformation, supposing it is caused by buckling due to an external compression force and the contribution of external transverse forces, such energy variation must be equal to the respective work variation by the external compression force over the associate displacement u_{axinlg},

$$\Delta U_{Strain} = \{\Delta y_e\}^T EI\left\{\int_0^{Le}[N''(x)]^T[N''(x)]dx\right\}\{y_e\} + \{\Delta y_e\}^T\{F_e\} = F_{Axial}\Delta u_{axnlg} \quad (12)$$

Substituting, the displacement variation leads to the matrix formula:

$$\Delta U_{Strain} = \{\Delta y_e\}^T EI\left\{\int_0^{Le}[N''(x)]^T[N''(x)]dx\right\}\{y_e\} - \{\Delta y_e\}^T\{F_e\} =$$
$$-\{\Delta y_e\}^T F_{Axial}\left\{\int_0^{L_0}[N'(x)]^T[N'(x)]dx\right\}\{y_e\} \quad (13)$$

Since the displacement variation is an arbitrary quantity, it can be removed from the above formulation. Consequently, the problem of beam bending under transverse loads and also considering the influence of non-linear geometric axial load, can be addressed independently.

$$\left\{EI\left[\int_0^{Le}[N''(x)]^T[N''(x)]dx\right]+F_{Axial}\left[\int_0^{L_0}[N'(x)]^T[N'(x)]dx\right]\right\}\{y_e\}=\{F_e\} \quad (14)$$

This matrix equation presents two significant components: the first representing the linear elastic stiffness matrix only for transverse bending forces and displacements, while the second one represents the non-linear geometric contribution due to an axial force. If the force, F_{Axial} is a tensile one, the beam element stiffness increases, on the other hand if the force F_{Axial} is negative the beam becomes more flexible.

An important scenario arises when the total stiffness matrix is zero, which points to beam instability and failure by buckling. This means the following numerical situation:

$$EI\left[\int_0^{Le}[N''(x)]^T[N''(x)]dx\right]+F_{Axial}\left[\int_0^{L_0}[N'(x)]^T[N'(x)]dx\right]=0 \quad (15)$$

There is an incremental change in term due to axial force in contrast to the other term.

$$u_{axn}=-\frac{1}{2}\int_0^{L_0}\left(\frac{dy}{dx}\right)^2dx \quad (16)$$

contains the squared beam displacement amplitude, y_{max}^2, then a variation of this value is $2y_{max}\,\Delta y_{max}$ and number "2" will cancel the one of (1/2) in deformation term ε_{nlg} above.

From this expression we can obtain the critical force F_{Axial}, determining the beam element instability. In the case of assembling multiple beam elements, the above equation becomes an eigenvalue problem, where the axial forces obtained as roots of the polynomial expression refer to the associate buckling modes, depending of the number of assembled elements.

The main objective of this theoretical excerpt is to clarify how a second order deformation associated with axial loads on beams can lead to bending by instability (buckling).

For illustrative purposes, let's consider a simply supported beam with length L. One end of the beam is axially fixed (though free to rotate), while the opposed one can be displaced solely along the beam axis. We can assume the beam transverse displacement of the beam as y(x),

$$y(x)=y_{max}\sin\left(\frac{\pi x}{L}\right) \quad (17)$$

The derivatives of this function are,

$$y'(x)=\left(\frac{\pi x}{L}\right)y_{max}\cos\left(\frac{\pi x}{L}\right) \quad (18)$$

$$y''(x)=-\left(\frac{\pi x}{L}\right)^2y_{max}\sin\left(\frac{\pi x}{L}\right) \quad (19)$$

By substituting these trigonometric expressions into the energy equation mentioned earlier and solving for F_{Axial}, it's obtained the basic Euler buckling load for a pinned beam subjected to an axial force F_{Axial} (representing the first critical load for the initial buckling mode),

$$F_{Axial}=\frac{\pi^2EI}{L^2} \quad (20)$$

4- FINITE ELEMENT ANALYSIS

As mentioned before, the crane model allows configurations which can vary between 21 m and 42 m in height for the tower and between 33 m and 60 m for the boom. For this specific case, the crane had

a boom with a length of 45 m and the tower was 60 m height (height not foreseen in the manual). For this boom length, it is specified that the ballast must be equal to 15 Ton (150 kN), consisted by 5 units of 2 tones (20 kN) plus two units of 1,5 tones (15 kN) each.

To understand the main causes for the collapse, a structural numerical analysis for the tower crane modules is performed under this configuration.

4.1. 3D computational model

The 3D model of the crane was design in the CAD program SolidWorks® [13], using data collected from the manufacturer manual and obtained from the structure whenever these dimensions were not available in the drawings. The detailed drawings of the tower crane are presented in Figure 16.

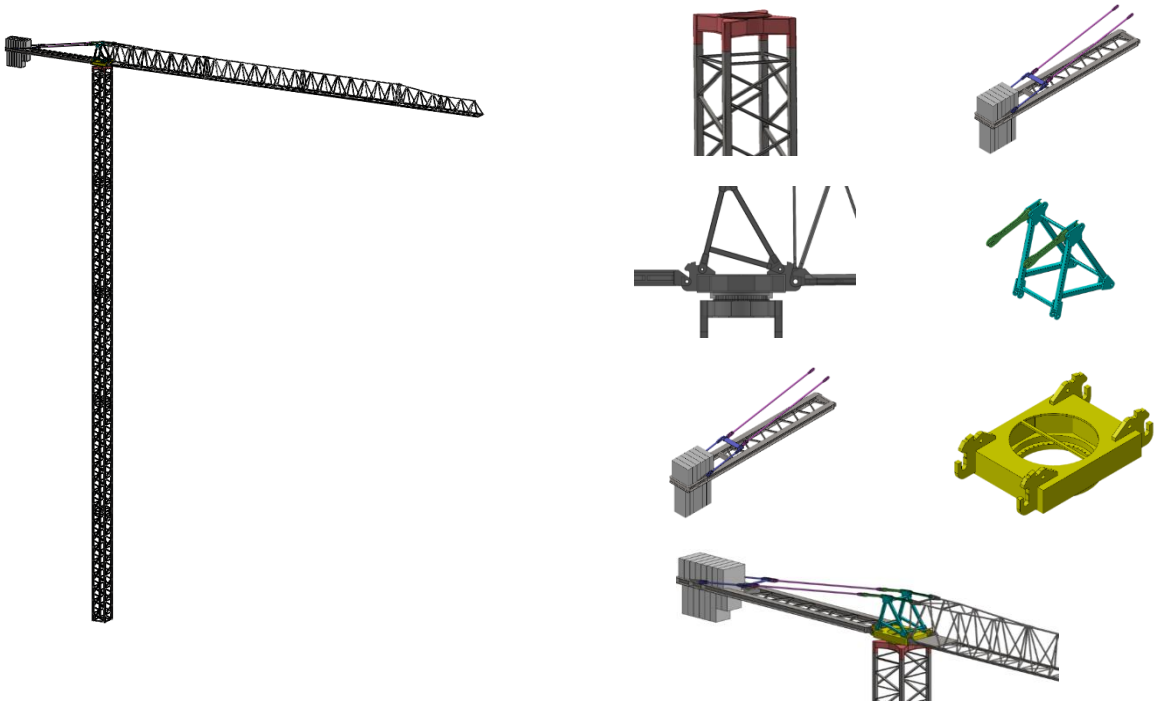

Fig. 16 | CAD 3D model (Solid Works®) of the tower crane and its several parts in detail.

4.1. Static Analysis

Numerical analyses were performed using finite element methods (FEM) formulations with Abaqus® software [14]. The tower crane model was meshed with 17270533 linear tetrahedral elements (C3D4) with 5237122 nodes (Figure 17).

The tower crane material is steel ($\rho = 7800\ kg/m^2$) and the model total mass is 44803 kg, representing an error of approximately 3,75% relative to the total mass provided by the manual (approximately 46,55 tones). Due to the model's lower mass compared to the one specified in the manual, the obtained results provide an assurance of safety, because the vibration frequencies decrease with the increasing of mass, ensuring a conservative approach in the analysis. The inertia properties for the tower crane are shown in Table 1.

The problem was modelled according to the real conditions, i.e., the effect of the ballast mass

Table 1 | Inertia properties of the crane relative to the origin [kg.m²].

$I_{xx} = 1.5E4$	$I_{xy} = 7.05E2$	$I_{xz} = 4.25E-2$
$I_{yz} = 7.05E2$	$I_{yy} = 4.51E3$	$I_{yz} = 7.16E-2$
I_{zx}	I_{zy}	$I_{zz} = 1.95E4$

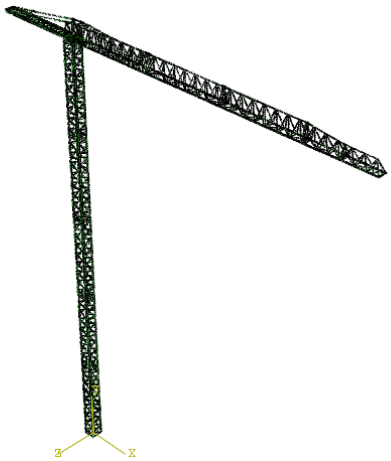

Fig. 17 | Discretized model: 17270533 tetrahedral elements and 5237122 knots (Abaqus®).

applied as a vertical load of 15 tons in the counter-boom (Figure 18 a)) and the boundary conditions as completely fixed - null rotations and translations - in the tower base foundation (Figure 18b)).

A static analysis was conducted, considering only the crane's weight. The manual provided by the manufacture stipulates specific allowable static values for the vertical load P, normal reaction Rh, and moment Mv based on the height in the case of a fixed tower (values are shown in the Table 2).

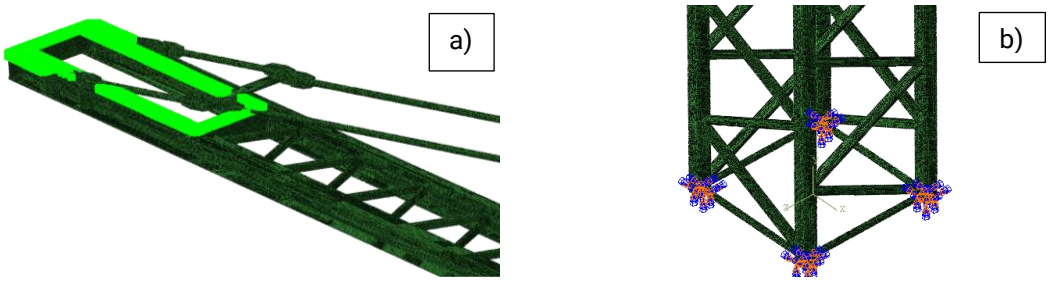

Fig. 18 | a) Vertical load of 15 tones applied in the counter-boom; b) Boundary condition – tower base: fixed.

Table 2 | Admissible values for vertical load, normal reaction and moment (according crane's manual).

$\boldsymbol{H}$ $[m]$	$\boldsymbol{M_v}$ $[kN.m]$	$\boldsymbol{P}$ $[kN]$	$\boldsymbol{R_h}$ $[kN]$
21	1041	358	26
24	1078	367	30
27	1111	375	34
30	1147	383	38
33	1188	390	42
36	1233	398	45
39	1281	406	49
42	1333	414	53

As already mention before, the manual for this particular crane model specifies vales exclusively for a maximum height of 42 m, and don´t for 60 m height - corresponding to the crane installed.

By fitting a function to the values provided for each of the three parameters as a function of height (Figure 19), it's possible to check that all of them vary linearly, being feasible to extrapolate each of these parameters to a height of 60 m. Performing a linear regression for each parameter where an equation is obtained, allowing the calculation of values corresponding to a height of 60 m.

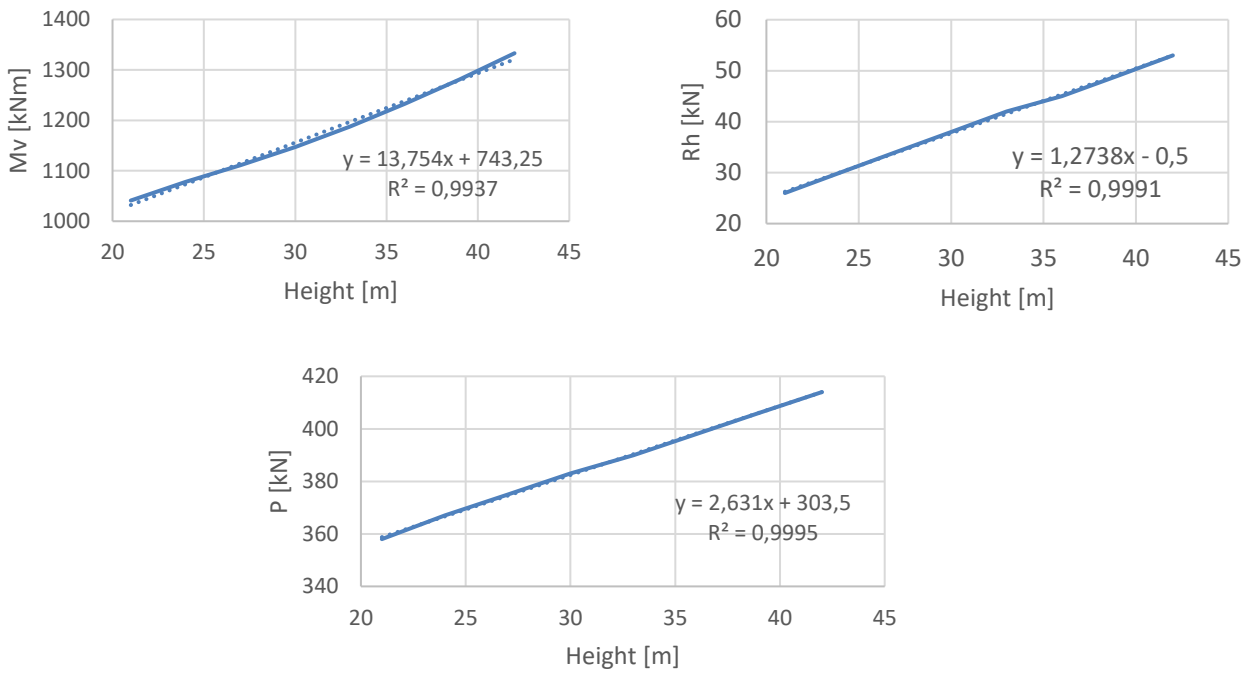

Fig. 19 | Relationship between the parameters (P, Rh, Mv) and the crane height.

Substituting the "x" for 60 m in each equation, it is possible to determine the maximum permissible values for static requests for a height of 60 m, yielding the following results:

$P = 461\ kN$
$R_h = 75\ kN$
$M_v = 1568\ kN.m$

Through a static simulation, the following value of $P = 448\ kN$ is calculated and the value of $Rh = 0\ N$. The values computed are below the maximum admissible values.

To estimate Mv, which is the moment generated by the eccentricity of the masses in each section of the crane's upper part (boom, counter-boom, pyramid and slewing unit), the eccentricity relative to each component center of mass need to be considered (Table 3). The moment Mv is calculated as follows:

$$M_v = -9{,}2 \times 18860 + 3{,}0 \times 5890 + 18{,}4 \times 1250 + 30{,}1 \times 1130 + 38{,}6 \times 465 + 43{,}7 \times 298 + 45 \times 1800 = 13\ kN.m \quad (21)$$

Table 3 | Position's center of mass and weight of each component.

	x [m]	**y** [m]	**Weight** [kg]
Counter boom + ballast	-9,2	61,2	18860
Boom 1+ Pyramid + Slewing Unit	3,0	61,5	5890
Boom 2	18,4	61,7	1250
Boom 3	30,1	61,8	1130
Boom 4	38,6	61,7	465
Boom 5	43,7	61,5	298
Maximum weight lifted at the end of the boom	45	-	1800

Therefore, based on static results obtained, the structure follows the manufacturer's specifications. However, considering the dimensions of the structure, its behavior must also account for dynamic requests. As an elastic structure, when subjected to loads which changes its balance, it may oscillate in its natural frequencies around the equilibrium position. These oscillations can be excited by any variable load acting on the structure, such as the action of the wind, any impact load or the pendular oscillations of suspended loads. When any of these factors coincide with the natural frequencies of the structure, it can lead to a resonance phenomenon characterized by an increasing in vibration amplitude. To avoid such situations, it's crucial to conduct a dynamic analysis, as structures whose natural frequencies can be excited during normal use should be avoided.

4.2. Dynamic analysis

The dynamic study is of fundamental importance for this type of structures, given their primary purpose of lifting and moving loads, often characterized by high masses that can vary cyclically due to the crane movement and the pendulum effect [15, 16]. Due to the internal oscillations, their elastic and external response and the different types of loads, the structure tends to oscillate around its equilibrium position. This type of vibration (like a pendulum) can cause instability and irreversible damage to the structure. These oscillations also generate forces of inertia that act on the connections and screws, exposing them to variable loads which can cause fatigue.

Mechanical vibration (oscillation) is defined as an alternating movement around a reference position. The frequency of oscillation of the natural movement of an elastic structure to an initial disturbance is known as its natural frequency:

$$natural\ frequency\ (\omega_n) = \sqrt{\frac{stiffness\ (k)}{weight\ (m)}} \tag{22}$$

When a mechanical system is excited at its natural frequency, the response of the system amplitude may be greater than the predicted by the project for a static load. Hence, it must be ensured that the frequencies excited by the load or wind are outside the natural frequency range of the structure or, if there is such a risk, increase the damping of the structure. The metallic structure of the crane, given its flexibility, is not very dampened, which is verified by the oscillations usually seen along the cargo handling.

The crane main characteristics are its low mass and flexibility, therefore when a substantial height increasing happens, the necessity for a dynamic study is essential. Knowing that the natural frequency decreases with an increase in weight, this effect is intensified when additional masses, such as counterweights or payloads, are added to the top of the structure. The same happens by increasing the flexibility, a characteristic which increases with the height of the structure, increasing the susceptibility to vibrations because it lowers the natural frequency.

In the present case, there was a significant increase in mass (compared to a crane with 42 m in height), decreasing the stiffness and consequently decreasing the value of the natural frequency. Thus, a dynamic simulation was performed using again Abaqus® software, with the same numerical model used in the static analysis but now configured for a dynamic analysis.

4.2.1. Dynamic analysis for a crane with 60 m height

The dynamic simulation allowed to obtain the first three natural frequencies of the structure and its respective modes. Figure 20 depicts the maximum deformation position during oscillation around the equilibrium.

The first natural frequency obtained was $f_1 = 0{,}1339\ Hz$. In the first eigenmode, the tower and the boom are decoupled and there are some torsion of the tower and flexing of the boom, which is easily observed when operating the crane by twisting the main body whenever the boom is moved in rotation (Figure 20 a). In the second eigenmode, the tower and the upperpart are coupled behaving like a rigid body with both having an upward movement, with an oscillation whose natural frequency is $f_2 = 0{,}1423\ Hz$ (Figure 20 b). In the third eigenmode, the boom twists and the tower bends, as in the first mode, but with a lower amplitude of response, $f_3 = 0{,}1589\ Hz$ (Figure 20 c). The second eigenmode obtained corresponds exactly to the real collapsing dynamics of the tower crane under study.

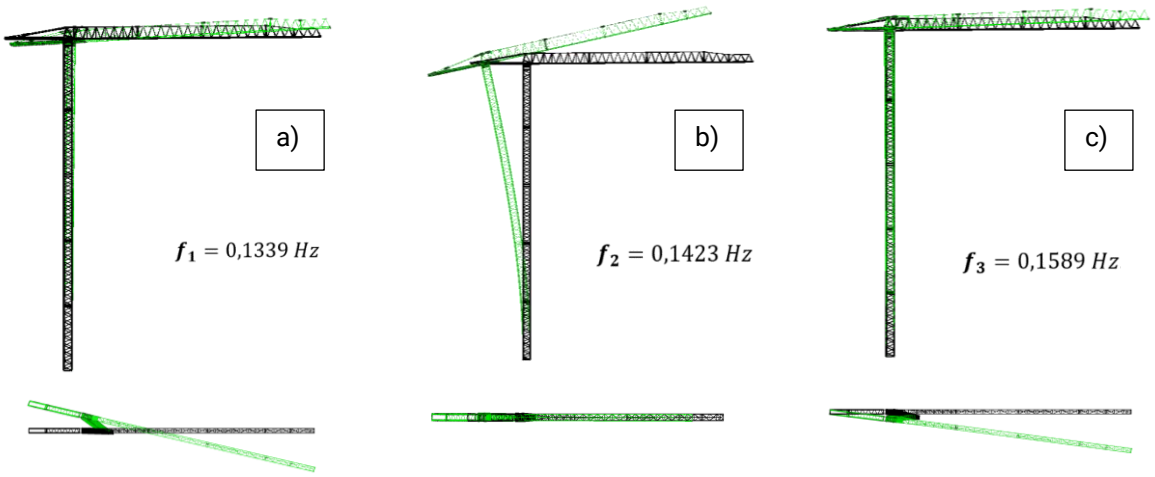

Fig. 20 | a) first eigenmode; b) second eigenmode; c) third eigenmode.

The crane's behavior is a coupled movement between the crane and the suspended load, considering that the load behaves like a pendulum when it oscillates, this effect dynamically excites the crane. In the gravitational pendulum, the frequency of oscillation is determined by the length of the suspension wire. Similarly, in the case of load movements, both the dimensions of the wire and the suspended mass vary (Figure 21), leading to the possibility of exciting different frequencies. Therefore, comparing the natural frequencies of the pendulum with those of the crane, it is possible to verify if there was the possibility of the crane being excited by the suspended load.

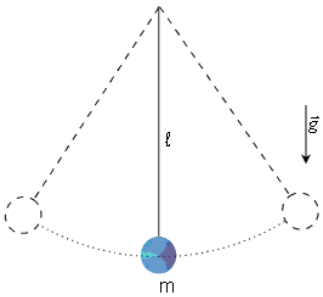

Fig. 21 | Gravitational Pendulum's.

$$T = 2\pi\sqrt{\frac{l}{g}} \qquad (24)$$

where "l" is the height of the pendulum and "g" represents the gravitational acceleration $g = 9{,}81\ m/s^2$.

By varying the value of "l" between 10 and 15 m, the values for the period (T) and frequency are obtained (Table 4).

Table 4 | Period and natural frequency values for a load suspension length between 10 and 15 m.

l [m]	T [s]	f [Hz]	Crane Mode
10	6,35	0,1576	Near 3rd mode (0,1589 Hz)
11	6,66	0,1502	Between 2nd and 3rd mode
12	6,95	0,1438	Near 2nd mode (0,1423 Hz)
13	7,24	0,1382	Between 1st and 2nd mode
14	7,51	0,1332	Close to 1st mode (0,1339 Hz)
15	7,77	0,1286	Close to 1st mode (0,1339 Hz)

The values obtained are very close to the three natural frequencies of the crane (0,1339 Hz; 0,1423 Hz; 0,1589 Hz), indicating that an oscillation in the suspended load can excite one of the crane natural frequencies. This can result in significantly high response amplitudes, potentially causing the crane to failure due to the inertia forces generated by the oscillation.

4.2.2. Dynamic analysis for a crane with 42 m height

In order to compare the values of the natural frequencies obtained for the 60 m model, the same dynamic simulation was performed to demonstrate that by reducing the height to 42 m as recommended in the manual, the first two natural frequencies, which are the easiest ones to excite, would increase, being therefore more difficult to occur and cause resonance of the crane structure. The first two natural frequencies obtained were $f_1 = 0{,}1985\ Hz$ and $f_2 = 0{,}2052\ Hz$ (Table 5).

Recalculating the natural frequencies for the suspended load (pendulum effect), the values close to these frequencies are obtained for lengths between 6 m and 7 m (Table 6), which are unlikely lengths for handling loads suspended on a crane of this dimension.

Table 5| A comparison between the first two natural frequencies for a crane's height of 42 m and 60 m.

	Crane frequency [Hz] **with 60 m height**	**Crane frequency** [Hz] **with 42 m height**	**Comparison**
f_1	0,1339	0,1985	33%
f_2	0,1423	0,2052	31%

Table 6| Period and natural frequency values for a pendulum with a length of 6 and 7 meters.

l [m]	T [s]	f [Hz]	**42 m crane's mode**
6	4,92	0,2034	Near 2nd mode (0,2052 Hz)
7	5,31	0,1883	Close to 1st mode (0,1883 Hz)

Whenever operating a crane at considerable heights while handling heavy loads, there is a risk of excitation its natural frequencies, consequently, it is crucial to dimension a crane dynamically in such scenarios. One approach is to employ more robust structures, characterized by increased rigidity and higher natural frequencies. Alternatively, and if feasible, it's using the crane tied to a neighboring structure, which helps to increase the natural frequencies by preventing vibration modes that could lead to significant displacements amplitudes.

5- CONCLUSIONS

The tower crane collapse presented in this paper was not caused by a single factor; rather it was due to a combination of circumstances that significantly increased the risk of collapse. On modifying the crane tower assembly to a higher height (60 m), more than the maximum allowable by the manual (42 m), this rendered the structure more flexible, decreasing its natural frequencies of vibration. Also, the inclusion of 15 tones counterweight (3 tones plus than the one recommended in the manual), contributed to reduce even more the vibration frequencies. Thus, whenever the natural frequencies were excited, the crane's oscillations increased, given its augmented flexibility, so generating dynamic loads on the bolted joint, which, due to its failure by fatigue, caused the accident.

Regarding the effect of axial loads leading to buckling in structures, the numerical formulation presented in this study demonstrates that once this effect initiates (due to structure imperfections or a combination of transverse loads, such as wind pressure), it rapidly propagates without control, often resulting in catastrophic consequences.

Static and dynamics numerical simulations were performed for the 60 meters tower crane height, and although it verified its static stability, it was found that the dynamic stability was compromised since it did not have enough stiffness, once the dynamic simulations showed that the crane involved in the accident had natural vibration frequencies that could be excited under normal conditions of operation. Moreover, the second eigenmode obtained corresponded exactly to the real collapsing dynamics of the tower crane.

Finally, it is recommended to include dynamic dimensioning to design this type of structures, due to the potential damage and failures that can occur from inertia-induced loads.

REFERENCES

[1] Bureau of Labor Statistics, "Crane-related occupational fatalities." (2008).

[2] “Tower Crane Incidents Worldwide” Health and Safety Laboratory, UK (2010);

[3] “Crane-Related Deaths in Construction and Recommendations for Their Prevention”, The Center for Construction Research and Training – NIOSH, USA (2008);

[4] Milazzo, M. F., et al. "Investigation of crane operation safety by analyzing main accident causes. "Risk, Reliability and Safety: Innovating Theory and Practice (2016);

[5] Ross, Bernard, Brian McDonald, and SE Vijay Saraf. "Big blue goes down. The Miller Park crane accident." Engineering Failure Analysis 14.6 (2007);

[6] Zrnic, Nenad D., et al. "Failure analysis of the tower crane counterjib." Procedia engineering 10 (2011);

[7] McDonald, Brian, Bernard Ross, and Robert A. Carnahan. "The Bellevue crane disaster." Engineering Failure Analysis 18.7 (2011);

[8] Swuste, Paul. "A 'normal accident' with a tower crane? An accident analysis conducted by the Dutch Safety Board." Safety science 57 (2013);

[9] Isherwood, R. "Tower crane incidents worldwide." (2010);

[10] Marquez, Anibal Angel, P. Venturino, and J. L. Otegui. "Common root causes in recent failures of cranes. "Engineering Failure Analysis 39 (2014);

[11] euro crane stability." London: CIRIA (2006);

[12] Standard, British. "Eurocode 3—Design of steel structures — "BS EN 1993-11 (2006);.

[13] Solidworks – Software CAD (computer-aided design);

[14] ANSYS Workbench – Software CAD for structural analysis;

[15] Ju, F., and Y. S. Choo. "Dynamics Characteristic of Tower Cranes." Structural Stability and Dynamics (2003);

[16] F. Ju, Y.S. Choo, F.S. Cui; "Dynamic response of tower crane induced by the pendulum motion of the payload" Singapore (2005);